Rectangular Waveguide With Dielectric-Filled Corrugations Supporting Backward Waves

Islam A. Eshrah, *Student Member, IEEE*, Ahmed A. Kishk, *Fellow, IEEE*, Alexander B. Yakovlev, *Senior Member, IEEE*, and Allen W. Glisson, *Fellow, IEEE*

***Abstract*—A new application for corrugated waveguides as left-handed (LH) meta-material guided-wave structures is investigated. The waveguide is operated below the cutoff of the dominant mode, where the waveguide has an inherent shunt inductance. The dielectric-filled corrugations are used to provide a series capacitance, which, along with the shunt inductance, create the necessary environment to support backward waves. A simple equivalent-circuit model is constructed, and proves quite accurate in determining the dispersion, as well as the scattering characteristics of the structure. Experimental verification of the occurrence of backward waves in the corrugated waveguide is presented. Very good agreement between the results obtained using the equivalent-circuit model and the full-wave finite-difference time-domain solution is achieved. The effect of the various design parameters on the LH propagation bandwidth is investigated. The advantages and possible applications of the structure are discussed.**

***Index Terms*—Corrugated waveguide, metamaterial transmission lines, moment methods, periodic structure.**

I. Introduction

WITH THE increasing interest in meta-material transmission lines (TLs) [1]–[4] that exhibit negative refraction resulting in left-handed (LH) propagation [5]–[11], attention was drawn toward guided-wave structures that manifest the same behavior [12]–[15]. Such structures have the advantage of being closed and, thus, have minimal radiation losses and do not suffer from any extraneous effects. In [13], an LH waveguide was realized by inserting printed split-ring resonators along the direction of propagation in the conventional rectangular waveguide. In terms of the TL equivalent-circuit model, the reason of using these insertions is to realize series capacitance and shunt inductance simultaneously within the frequency range in which LH propagation is desired.

In this paper, the series capacitance is achieved by introducing dielectric-filled transverse corrugations to the waveguide broad wall, as shown in the geometry in Fig. 1. Corrugated waveguides have been traditionally used with corrugated horn antennas [16] to support hybrid modes that improve the radiation characteristics. With the proper choice of the corrugation parameters, however, they can serve as a capacitive immittance surface instead. Operating the waveguide below the cutoff frequency, where an inherent shunt inductance occurs, in the presence of the capacitive corrugations provides the required environment for supporting the LH propagation regime.

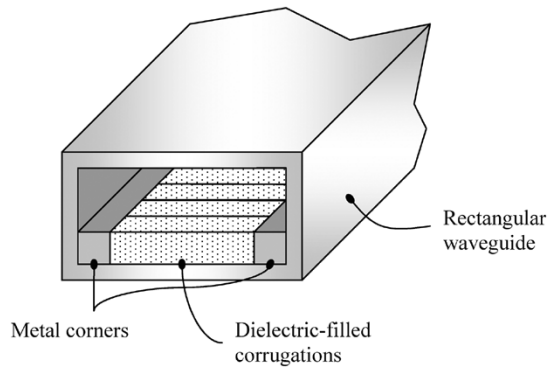

Fig. 1. Rectangular waveguide with dielectric-filled corrugations supporting LH propagation.

In [14], a brief description of the analysis of the corrugated waveguide using an equivalent TL model was discussed. The analysis was based on determining the per-unit-length parameters of the equivalent TL model and identifying the passband and stopband. In addition to the simple circuit model that can accurately predict the behavior of the structure, a full-wave modal solution of this waveguide was performed in [15], where spectral analysis of the infinite periodically corrugated waveguide is presented and the dispersion characteristics of the structure were investigated.

In Section II, the circuit model of the unit cell, i.e., one corrugation, is presented in detail. From the circuit analysis, the propagation constant is estimated. Experimental results illustrating the occurrence of LH propagating waves are presented in Section III, along with results showing the phase advance phenomenon. The effect of the various parameters on the bandwidth of the LH operation is also presented in Section III. The results obtained using the circuit analysis are compared to those obtained using the finite-difference time-domain (FDTD) method and exhibit very good agreement. Conclusions and discussions are presented in Section IV.

II. Equivalent-Circuit Model

The physical and electrical parameters of the corrugated waveguide are given in Fig. 2. The waveguide is assumed to be air filled, i.e., $\mu = \mu_0$ and $\varepsilon = \varepsilon_0$. The corrugation length l_s does not necessarily have a wall-to-wall extent, i.e., $l_s \leq a$. The corrugations are filled with a material having constitutive parameters μ_s and ε_s, and have width, depth, and period w_s, t_s,

Manuscript received March 31, 2005; revised May 23, 2005. This work was supported in part by the Army Research Office under Grant DAAD19-02-1-0074.

The authors are with the Department of Electrical Engineering, The University of Mississippi, University, MS 38677 USA (e-mail: ieshrah@olemiss.edu; ahmed@olemiss.edu; yakovlev@olemiss.edu; aglisson@olemiss.edu).

Digital Object Identifier 10.1109/TMTT.2005.855748

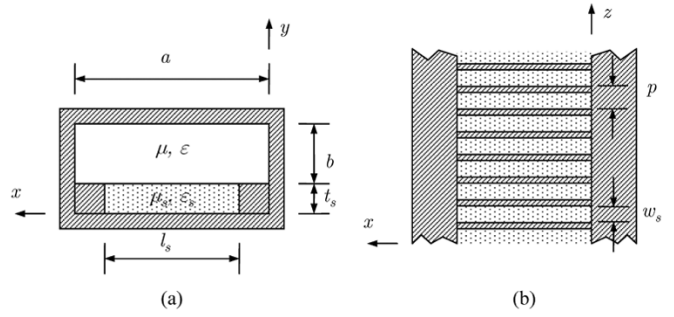

Fig. 2. Rectangular waveguide with dielectric-filled corrugations. (a) Transverse section. (b) Longitudinal (top) section.

and p, respectively. The waveguide height b is measured from the corrugation interface to the other wall of the waveguide.

The TL or telegrapher's equations for the modal voltage and current of the conventional rectangular waveguide [17] imply that the equivalent circuit of a differential TL element depends on the mode type (TE or TM) and the mode state (propagating or evanescent) [14]. For the dominant TE_{10} mode of the waveguide, the TL equations may be written as

$$\frac{dV}{dz} = -j\omega L' I \quad \frac{dI}{dz} = -j\omega C' V \tag{1}$$

where L' and C' are the per-unit-length inductance and capacitance of the equivalent TL, respectively, and may be expressed as

$$L' = \mu \frac{Z_0}{\eta} \quad C' = \varepsilon \frac{\eta}{Z_0} \left(1 - \left(\frac{f_c}{f}\right)^2\right) \tag{2}$$

where $\eta = \sqrt{\mu/\varepsilon}$, f_c is the cutoff frequency of the waveguide dominant mode, and the impedance Z_0 is constant and depends on the adopted definition of the waveguide characteristic impedance. For the power–voltage definition of the waveguide characteristic impedance [18], Z_0 is given by

$$Z_0 = 2\eta \left(\frac{b}{a}\right). \tag{3}$$

It can be readily seen from (2) that, above the cutoff frequency, the conventional series L shunt C model is obtained. Below the cutoff, however, a series L shunt L circuit model reflects the evanescent nature of the TE mode since C' becomes negative for $f < f_c$. Thus, an inherent shunt inductance occurs for the evanescent TE mode. To realize the series C shunt L circuit model that supports LH propagation, a capacitive series waveguide discontinuity is required. Transverse broad wall slots, which are known to be modeled as series loads, may be loaded with a capacitive impedance to yield the required series capacitance.

One possible load that satisfies this requirement is a short-circuited waveguide section with cross-sectional dimensions equal to that of the slot. To support propagating waves and have a cutoff frequency less than that of the waveguide, the short-circuited waveguide should be filled with a dielectric with sufficiently high permittivity. The slot with the short-circuited section can be regarded as a dielectric-filled corrugation depicted

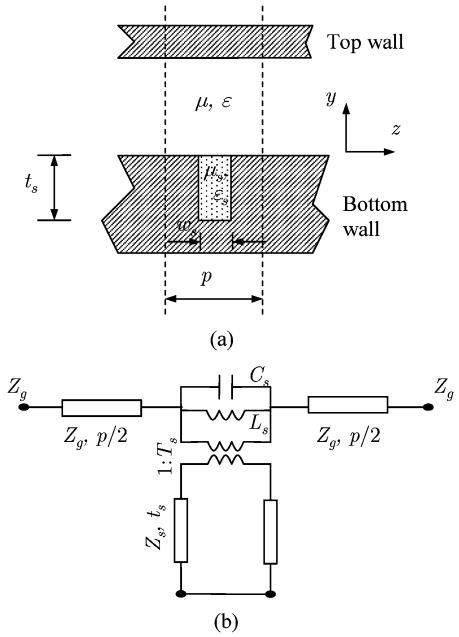

Fig. 3. Transverse slot loaded with a short-circuited waveguide section. (a) A cut through one corrugated cell. (b) Equivalent-circuit model.

in Fig. 3(a). A simple equivalent-circuit model for waveguide transverse slots was constructed in [19] and, thus, the equivalent-circuit model of the corrugation may be obtained as depicted in Fig. 3(b). The *LC* parallel combination in Fig. 3(b) models the slot, whereas the transformer accounts for the change in impedance definition from the main waveguide to the secondary waveguide of the corrugation.

Thus, the admittance introduced by one corrugation may be given by

$$Y_{\mathrm{corr}} = j\omega C_s + \frac{1}{j\omega L_s} + \frac{\cot(\beta_s t_s)}{jT_s^2 Z_s} \tag{4}$$

where β_s and Z_s are the propagation constant and the characteristic impedance of the corrugation waveguide. For sufficiently narrow slots and sufficiently small period of the corrugations, i.e., $w_s < p \ll \lambda_g$, the effective per-unit-length inductance and capacitance of the TL model of the corrugated waveguide may be found using

$$C'_{\mathrm{eff}} = C' \quad L'_{\mathrm{eff}} = L' - \frac{j}{\omega p Y_{\mathrm{corr}}}. \tag{5}$$

Within some frequency range higher than the corrugation waveguide cutoff and lower than the main waveguide cutoff, and with the proper choice of the corrugation depth and period, C'_{eff} and L'_{eff} are negative corresponding to a shunt inductance and series capacitance, respectively. The typical behavior of the per-unit-length effective parameters is depicted in Fig. 4. It is clear that below the cutoff frequency f_c, C'_{eff} is negative, yielding a shunt inductance. Within the frequency range $f_{\Gamma 1} < f < f_{\Gamma 2}$ where the contribution of the capacitance provided by the corrugation exceeds that of the waveguide inductance, a series capacitance is achieved and, thus, LH propagation can be supported. Whereas Fig. 4 shows the case where $f_{\Gamma 1} < f_{\Gamma 2} < f_c$, different dimensions may result

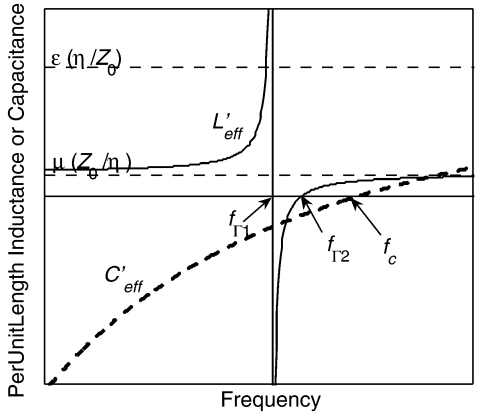

Fig. 4. Typical curves for the effective per-unit-length inductance and capacitance of the TL model. The scale of the inductance and capacitance is not the same.

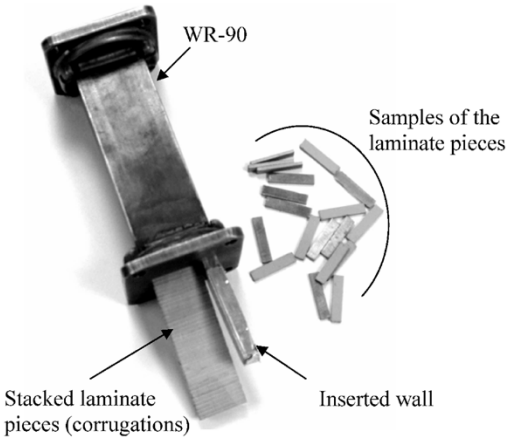

Fig. 5. Manufactured corrugated waveguide prototype showing the artificial conducting wall, the corrugations inserted in the waveguide, and some pieces of the laminate before stacking them to form the corrugations.

in $f_{\Gamma 1} < f_c < f_{\Gamma 2}$. The propagation constant may thus be computed in the different frequency ranges using

$$\beta = \begin{cases} \omega\sqrt{L'_{\rm eff}C'_{\rm eff}}, & f > f_{\rm RH} \\ -\omega\sqrt{L'_{\rm eff}C'_{\rm eff}}, & f_{\Gamma 1} < f < f_{\rm LH} \\ -j\omega\sqrt{|L'_{\rm eff}C'_{\rm eff}|}, & \text{elsewhere.} \end{cases} \tag{6}$$

where $f_{\rm RH} = \max\{f_c, f_{\Gamma 2}\}$ and $f_{\rm LH} = \min\{f_c, f_{\Gamma 2}\}$. In (6), the first and second branches correspond to right-handed (RH) and LH propagation, respectively, and the third branch corresponds to evanescence occurring when the per-unit-length parameters have opposite signs. Alternatively, the propagation constant may be obtained using the Bloch–Floquet theorem as

$$\beta = \frac{1}{p}\cos^{-1}\left(1 - \frac{\omega^2 p^2 L'_{\rm eff}C'_{\rm eff}}{2}\right). \tag{7}$$

Notice that (6) is the first-order approximation of (7) for a sufficiently small period. The frequencies $f_{\Gamma 1}$ and $f_{\Gamma 2}$ can be computed by letting $L'_{\rm eff}$ go to $-\infty$ and 0, respectively, yielding

$$Y_{\rm corr}(f_{\Gamma 1}) = 0 \quad Y_{\rm corr}(f_{\Gamma 2}) = \frac{-1}{j\omega_{\Gamma 2}L'} \tag{8}$$

which can be solved for these two frequencies numerically.

It is important to notice that for relatively electrically long slots that have wall-to-wall extent, the effect of the slot admittance is dominated by the short-circuit waveguide admittance. Moreover, the transformer turns ratio is unity. This facilitates the analysis of the structure even more, alleviates the need of determining the slot circuit parameters, and hence, helps speed up the design procedure using the circuit model.

III. Results

A. Verifications and Experimental Results

To verify the wave propagation below the cutoff, a prototype of the corrugated waveguide was realized as shown in Fig. 5. The corrugations were built by stacking rectangular pieces milled off a Rogers high-frequency laminate (RO3010) having a dielectric constant of $\varepsilon_{rs} = 10.2$ and thickness of $w_s = 1.27$ mm. The rectangles have dimensions of $l_s = 17$ mm and $t_s = 3.7$ mm. An artificial wall was inserted in a standard

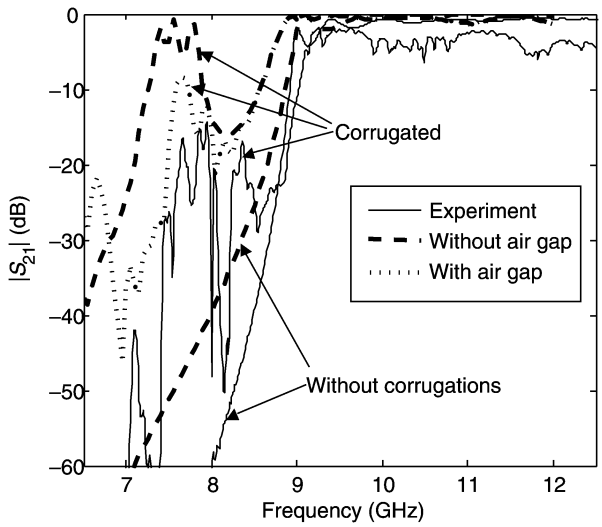

Fig. 6. Insertion loss for a rectangular waveguide with and without the corrugations. The simulation results are plotted for the cases with and without an air gap between the corrugation and bottom wall.

X-band waveguide section of length 8.8 mm to reduce the width to $a = 17$ mm and raise the cutoff frequency to $f_c = 8.82$ GHz. Fig. 6 shows the measured insertion loss with and without the corrugations. Experimental results are compared with those obtained using FDTD commercial software.[1] The waveguide is excited using standard X-band adapters connected to an HP8510 network analyzer.

The discrepancies between the experimental and simulation results are attributed to the imperfections in the hand-assembly manufacturing process of this simple prototype, namely, the air gap between the laminate pieces and the bottom wall of the waveguide, which is very crucial in the operation of the structure since it is based on the fact that the corrugations are short circuited. The effect of the air gap on the transmission coefficient is also shown in Fig. 6, where the simulation results with and without an air gap of 0.1 mm are depicted. Other sources

[1]QuickWave3D: A General Purpose Electromagnetic Simulator Based on Conformal Finite-Difference Time-Domain Method, ver. 2.2, QWED Sp. Z o.o, Warsaw, Poland, Dec. 1998.

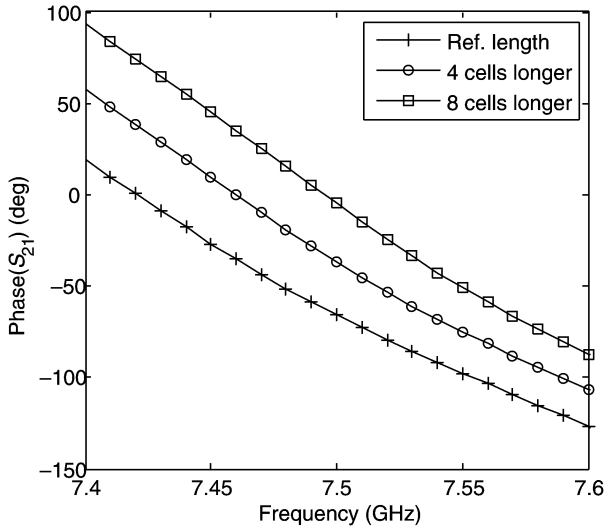

Fig. 7. Comparison between the phase of the transmission coefficient S_{21} of a reference waveguide section and a longer section.

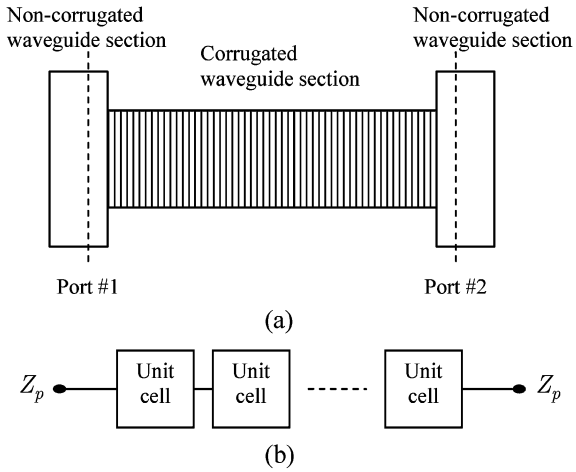

Fig. 8. Corrugated waveguide excited by an incident TE_{10} mode of a wider noncorrugated waveguide. (a) Original geometry. (b) Equivalent-circuit model.

of discrepancy include the possible nonuniform air gap between the corrugations and the artificial wall inserted in the waveguide and the air gaps between the corrugations themselves.

It is worth mentioning that the effect of the dielectric and conductor losses was taken into consideration in the FDTD simulation. That is why the transmission in the LH band experiences some attenuation, which is dominated by the dielectric losses (a loss tangent of 0.0023 at 10 GHz). For lossless dielectric, total transmission is observed in the LH band. The ripples in the transmission bands are due to the mismatch between the waveguide ports and the corrugated waveguide section, which results in standing waves that vary the response of the system with frequency.

To verify the phase advance phenomenon within the LH propagation band, the method suggested in [13] is employed, where the phase of the transmission coefficient S_{21} for a reference waveguide section is compared to that obtained for slightly longer sections having four and eight more cells. The phase advance over a portion of the LH band is plotted in Fig. 7, as obtained from the simulation. Notice the linear increase in phase with the increase in the number of cells at every frequency point.

B. Bandwidth Control and Parametric Studies

The effect of the various design parameters on the LH propagation bandwidth and dispersion characteristics is studied by considering the setup shown in Fig. 8(a) for which the equivalent circuit is depicted in Fig. 8(b). The broad wall of the port waveguides and the corrugated waveguide measure 22.86 and 17 mm, respectively. In the equivalent-circuit model, the ports are designated by the characteristic impedance Z_p. Every unit cell in Fig. 8(b) is made of the circuit in Fig. 3(b). Notice that the discontinuity is not modeled in the circuit model.

First, the effect of the waveguide height-to-width ratio b/a is investigated. Figs. 9 and 10 show that the bandwidth increases as the air-filled height b decreases. This can be explained in terms of equivalent-circuit model as the per-unit-length inductance L'

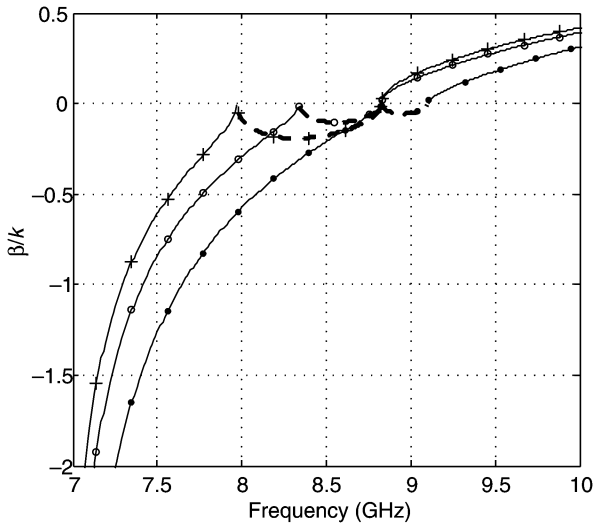

Fig. 9. Effect of the waveguide height b on the dispersion behavior of the corrugated waveguide. The solid and dashed lines represent the real and imaginary parts, respectively. The curves are plotted for b (mm) $= 6.46, 4.46,$ and 2.46 designated by $(+)$, $(\circ)$, and $(\bullet)$, respectively.

decreases and, thus, L'_{eff} will change its sign over a wider frequency range. In Fig. 9, the upper frequency $f_{\Gamma 2}$ of the LH band increases as b/a decreases, whereas the lower frequency $f_{\Gamma 1}$ is the same. Notice that the stopband $f_{\Gamma 2} < f < f_c$ tends to decrease as b/a decreases, approaching a balanced condition for the composite waveguide [4], i.e., $f_{\mathrm{RH}} = f_{\mathrm{LH}}$. Indeed, at $b = 2.75$ mm, $f_{\Gamma 2} = f_c$, resulting in a vanishing bandgap. For lower values of b, $f_{\Gamma 2}$ is greater than f_c, which causes the LH passband to occur in the range $f_{\Gamma 1} < f < f_c$, the RH passband in the range $f > f_{\Gamma 2}$, and the stopband in the range $f_c < f < f_{\Gamma 2}$, as observed in the case with $b = 2.46$ mm in Fig. 9. The narrow stopband in this case results in a smoother transition from the LH to RH passbands, as shown in Fig. 10(b), compared to the case depicted in Fig. 10(a). The plots in Fig. 10 also show a comparison between the circuit model results obtained using Agilent's Advanced Design System (ADS) [20] and the full-wave FDTD results obtained using Quickwave 3-D.

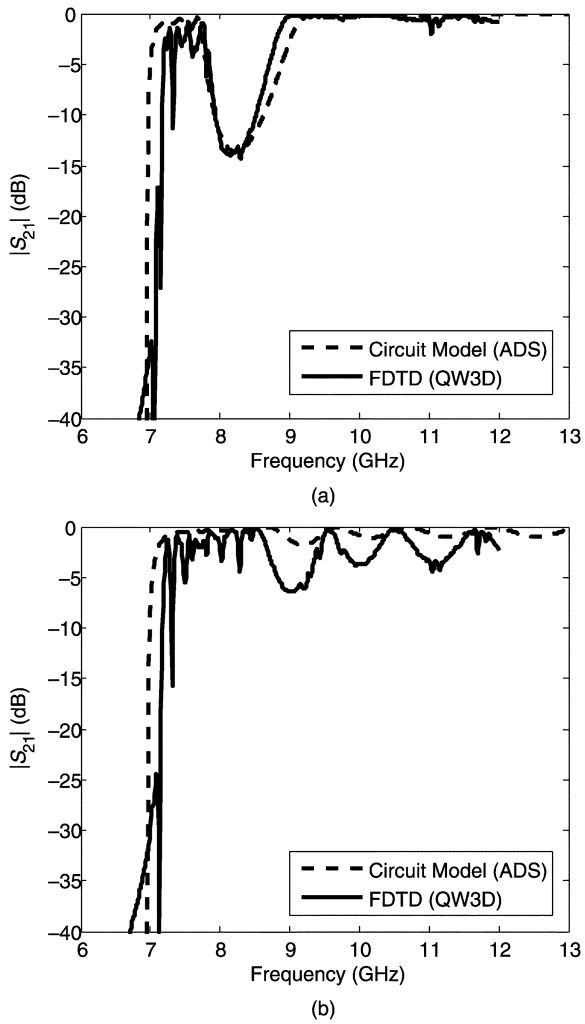

Fig. 10. Effect of the waveguide height b on the transmission coefficient S_{21}. (a) $b = 6.46$ mm. (b) $b = 2.46$ mm.

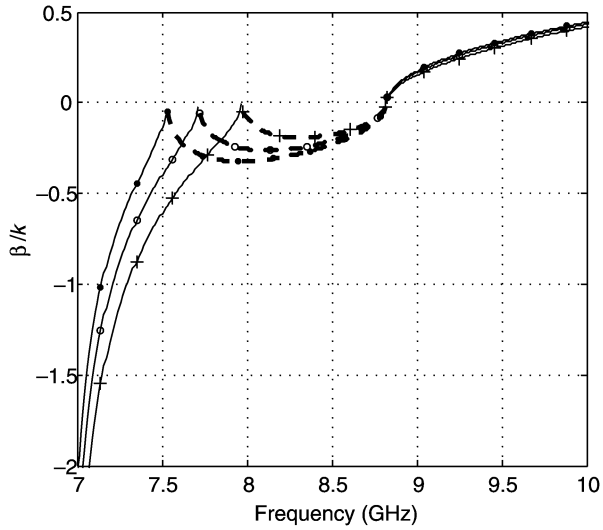

Fig. 11. Effect of the corrugations width-to-period ratio on the dispersion behavior of the corrugated waveguide. The solid and dashed lines represent the real and imaginary parts, respectively. The curves are plotted for $w_s = 1.27$ mm, and p (mm) $= 1.37, 1.905$, and 2.54 designated by $(+)$, $(\circ)$, and $(\bullet)$, respectively.

An increase in the corrugation width for a fixed period is reflected positively on the bandwidth, as depicted in Fig. 11. This can be expected since the average capacitance offered by the corrugations increases as w_s/p increases. However, for a constant width-to-period ratio, varying the period has virtually no effect on the dispersion characteristics, provided that the narrow slot approximation is not violated and the period is small relative to the wavelength. This can be understood from the expression of L'_{eff} where the term pY_{corr} is a function of the width-to-period ratio.

Decreasing the length of the corrugation l_s results in an increase in the corrugation waveguide cutoff frequency and, thus, an increase in the corrugation wavelength λ_s. This results in a decrease in the corrugation electrical depth t_s/λ_s and, consequently, a positive shift in the LH band. Also, since the corrugation characteristic impedance increases as l_s decreases, the capacitive susceptance of Y_{corr} decreases, and thus, the bandwidth of the LH operation decreases for shorter corrugations.

IV. Conclusion

A circuit model analysis for a rectangular waveguide with dielectric-filled corrugations was presented. The results obtained using the equivalent-circuit model, being in very good agreement with the full-wave FDTD solution, show that this structure can support LH propagation and predict with high accuracy its frequency band.

The simplicity of the analysis of this structure makes it an attractive tool to gain more insight into the physics of the LH propagation phenomenon in guided-wave structures, especially since the modal solution of the corrugated waveguide is available. The possibility of designing a dual-band LH waveguide by using corrugations with different depths either on opposite walls or alternating on the same wall was also considered. It is also interesting to notice that the dimensions of the waveguide may be miniaturized while supporting the LH propagating waves.

An interesting potential application for the composite RH/LH waveguide is its use in waveguide slot antenna arrays, where the scanning capability can be improved by frequency scanning through the RH and LH passbands. A well-known problem for waveguide antenna arrays is the fact that the waveguide wavelength is larger than the free-space wavelength. Thus, the elements are separated by a distance larger than half the free-space wavelength (to guarantee equiphase excitation), which may lead to the appearance of grating lobes while scanning the frequency. In the LH band, the guided propagation constant can be equal to or larger than its free-space counterpart (in magnitude) and its gradient with frequency is much higher, allowing large scan angles with small frequency change. This alleviates the need to use elements with wide radiation pattern bandwidth since a small frequency sweep causes a large change in the propagation constant and, thus, a wide range of progressive phase shift between the array elements. The waveguide slots may be on the broad wall opposite to the corrugated wall or the narrow wall in the case of a two-walled corrugated waveguide.

Future study involves deeper investigation of the analysis of this periodic structure and understanding the behavior of the supported modes within this environment. Although this structure may be rather difficult to fabricate as compared to

other designs, such as split-ring resonator insertions in rectangular waveguide, it triggers the analysis of other structures that may exhibit the same effect including printed dipoles and slots, dielectric slabs with holes, strip-loaded dielectric slabs, and printed dipoles with vias.

ACKNOWLEDGMENT

The authors wish to thank the Rogers Corporation, Chandler, AZ, for providing a free sample of the high-frequency laminate under the Rogers University Program.

REFERENCES

[1] G. V. Eleftheriades, A. K. Iyer, and P. C. Kremer, "Planar negative refractive index media using periodically *L–C* loaded transmission lines," *IEEE Trans. Microw. Theory Tech.*, vol. 50, no. 12, pp. 2702–2712, Dec. 2002.

[2] G. V. Eleftheriades, O. Siddiqui, and A. K. Iyer, "Transmission line models for negative refractive index media and associated implementations without excess resonators," *IEEE Microw. Wireless Compon. Lett.*, vol. 13, no. 2, pp. 51–53, Feb. 2003.

[3] T. Decoopman, O. Vanbésien, and D. Lippens, "Demonstration of a backward wave in a single split ring resonator and wire loaded finline," *IEEE Microw. Wireless Compon. Lett.*, vol. 14, no. 11, pp. 507–509, Nov. 2004.

[4] A. Lai, C. Caloz, and T. Itoh, "Composite right/left-handed transmission line metamaterials," *IEEE Micro*, vol. 5, no. 3, pp. 34–50, Sep. 2004.

[5] V. G. Veselago, "The electrodynamics of substances with simultaneously negative values of ε and μ," *Sov. Phys.–Usp.*, vol. 10, no. 4, pp. 509–514, 1968.

[6] J. B. Pendry, "Negative refraction makes a perfect lense," *Phys. Rev. Lett.*, vol. 85, no. 18, pp. 3966–3969, 2000.

[7] D. R. Smith, W. J. Padilla, D. C. Vier, S. C. Nemat-Nasser, and S. Shultz, "Composite medium with simultaneously negative permeability and permittivity," *Phys. Rev. Lett.*, vol. 84, no. 18, pp. 4184–4187, 2000.

[8] N. Engheta, "An idea for thin subwavelength cavity resonators using metamaterials with negative permittivity and permeability," *IEEE Antennas Wireless Propag. Lett.*, vol. 1, no. 1, pp. 10–13, Dec. 2002.

[9] A. Alù and N. Engheta, "Pairing an epsilon-negative slab with a mu-negative slab: Resonance, tunneling and transparency," *IEEE Trans. Antennas Propag.*, vol. 51, no. 10, pp. 2558–2571, Oct. 2003.

[10] R. A. Shelby, D. R. Smith, and S. Shultz, "Experimental verification of a negative index of refraction," *Science*, vol. 292, no. 5514, pp. 77–79, 2001.

[11] J. B. Pendry, A. J. Holden, D. J. Robbins, and W. J. Stewart, "Magnetism from conductors and enhanced nonlinear phenomena," *IEEE Trans. Microw. Theory Tech.*, vol. 47, no. 11, pp. 2075–2081, Nov. 1999.

[12] R. Marques, J. Martel, F. Mesa, and F. Medina, "Left-handed-media simulation and transmission of EM waves in subwavelength split-ring-resonator-loaded metallic waveguides," *Phys. Rev. Lett.*, pp. 183 901–183 904, Oct. 2002.

[13] S. Hrabar, J. Bartolic, and Z. Sipus, "Waveguide miniaturization using uniaxial negative permeability metamaterial," *IEEE Trans. Antennas Propag.*, vol. 53, no. 1, pp. 110–119, Jan. 2005.

[14] I. A. Eshrah, A. A. Kishk, A. B. Yakovlev, and A. W. Glisson, "Evanescent rectangular waveguide with corrugated walls: A composite right/left-handed metaguide," in *IEEE MTT-S Int. Microwave Symp. Dig.*, 2005 [CD ROM].

[15] ——, "Modal analysis of corrugated rectangular waveguides supporting left-hand propagation," in *IEEE AP-S Int. Symp. Dig.*, 2005 [CD ROM].

[16] P. J. B. Clarricoats and A. D. Olver, *Corrugated Horns for Microwave Antennas*. London, U.K.: Peregrinus, 1984.

[17] N. Marcuvitz, *Waveguide Handbook*. London, U.K.: Peregrinus, 1986.

[18] P. A. Rizzi, *Microwave Engineering: Passive Circuits*. Englewood Cliffs, NJ: Prentice-Hall, 1988.

[19] I. A. Eshrah, A. A. Kishk, A. B. Yakovlev, and A. W. Glisson, "Load-independent equivalent circuit model for transverse waveguide slots," in *IEEE AP-S Int. Symp. Dig.*, 2005 [CD ROM].

[20] *Advanced Design System 2003A, User's Guide*, Agilent Technol., Palo Alto, CA, 2003.

Islam A. Eshrah (S'00) was born in Cairo, Egypt, in 1977. He received the B.Sc. and M.Sc. degrees in electronics and telecommunications engineering from Cairo University, Cairo, Egypt, in 2000 and 2002, respectively, and is currently working toward the Ph.D. degree in electrical engineering at The University of Mississippi, University.

From 2000 to 2002, he was a Teaching Assistant with the Department of Electronics and Telecommunications Engineering, Cairo University. His research interests include dielectric-resonator antennas, integral-equation numerical methods, modeling of microwave structures, phased-array systems, and metamaterial guided-wave structures.

Mr. Eshrah is a member of Phi Kappa Phi. He was the recipient of the 2004 Young Scientist Award presented at the URSI International Symposium on Electromagnetics, Pisa, Italy, the 2005 Young Scientist Award presented at the URSI General Assembly, New Delhi, India, and the 2005 Raj Mittra Junior Researcher Award presented at the Antennas and Propagation Symposium, Washington DC.

Ahmed A. Kishk (S'84–M'86–SM'90–F'98) received the B.S. degree in electrical engineering from Cairo University, Cairo, Egypt, in 1977, the B.S. degree in applied mathematics from Ain-Shams University, Cairo, Egypt, in 1980, and the M.Eng. and Ph.D. degrees in electrical engineering from the University of Manitoba, Winnipeg, MB, Canada, in 1983 and 1986, respectively.

From 1977 to 1981, he was a Research Assistant and an Instructor with the Faculty of Engineering, Cairo University. From 1981 to 1985, he was a Research Assistant with the Department of Electrical Engineering, University of Manitoba. From December 1985 to August 1986, he was a Research Associate Fellow with the same department. In 1986, he joined the Department of Electrical Engineering, The University of Mississippi, University, as an Assistant Professor. He was on sabbatical leave with Chalmers University of Technology during the 1994–1995 academic year. He is currently a Professor with The University of Mississippi (since 1995). He was an Editor (1997) and Editor-in-Chief (1998–2001) of the *ACES Journal*. He was the Chair of the Physics and Engineering Division, Mississippi Academy of Science (2001–2002). He has authored or coauthored over 150 refereed journal papers and book chapters. He coauthored *Microwave Horns and Feeds book* (London, U.K.: IEE, 1994; Piscataway, NJ: IEEE Press, 1994) and coauthored Chapter 2 of *Handbook of Microstrip Antennas* (Stevenage, U.K.: Peregrinus, 1989). His research interest includes the design of millimeter frequency antennas, feeds for parabolic reflectors, dielectric-resonator antennas, microstrip antennas, soft and hard surfaces, phased-array antennas, and computer-aided design for antennas.

Dr. Kishk is a member of Sigma Xi, the U.S. National Committee of International Union of Radio Science (URSI) Commission B, the Applied Computational Electromagnetics Society, the Electromagnetic Academy, and Phi Kappa Phi. He is currently an editor of the *IEEE Antennas and Propagation Magazine*. He was the recipient of the 1995 Outstanding Paper Award for a paper published in the *Applied Computational Electromagnetic Society Journal*. He was the recipient of the 1997 Outstanding Engineering Educator Award presented by Memphis Section of the IEEE. He was the recipient of the Outstanding Engineering Faculty Member of 1998. He was the recipient of the 2001 Faculty Research Award for outstanding performance in research and the 2005 School of Engineering Senior Faculty Research Award. He was also the recipient of the Valued Contribution Award for Outstanding Invited Presentation, "EM Modeling of Surfaces with STOP or GO Characteristics—Artificial Magnetic Conductors and Soft and Hard Surfaces" presented by the Applied Computational Electromagnetic Society. He was the recipient of the 2004 IEEE Microwave Theory and Techniques Society (IEEE MTT-S) Microwave Prize.

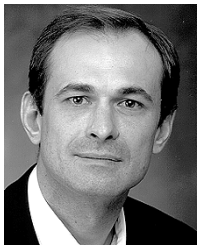

Alexander B. Yakovlev (S'94–M'97–SM'01) was born on June 5, 1964, in the Ukraine. He received the Ph.D. degree in radiophysics from the Institute of Radiophysics and Electronics, National Academy of Sciences, Kharkov, Ukraine, in 1992, and the Ph.D. degree in Electrical Engineering from the University of Wisconsin at Milwaukee, in 1997.

From 1992 to 1994, he was an Assistant Professor with the Department of Radiophysics, Dniepropetrovsk State University, Dniepropetrovsk, Ukraine. From 1994 to 1997, he was a Research and Teaching Assistant with the Department of Electrical Engineering and Computer Science, University of Wisconsin at Milwaukee. From 1997 to 1998, he was a Research and Development Engineer with the Compact Software Division, Ansoft Corporation, Paterson, NJ, and with the Ansoft Corporation, Pittsburgh, PA. From 1998 to 2000, he was a Post-Doctoral Research Associate with the Electrical and Computer Engineering Department, North Carolina State University, Raleigh. In Summer 2000, he joined the Department of Electrical Engineering, The University of Mississippi, University, as an Assistant Professor, and became an Associate Professor in Summer 2004. His research interests include mathematical methods in applied electromagnetics, modeling of high-frequency interconnection structures and amplifier arrays for spatial and quasi-optical power combining, integrated-circuit elements and devices, theory of leaky waves, and singularity theory.

Dr. Yakovlev is a member of URSI Commission B. He was the recipient of the 1992 Young Scientist Award presented at the URSI International Symposium on Electromagnetic Theory, Sydney, Australia, and the 1996 Young Scientist Award presented at the International Symposium on Antennas and Propagation, Chiba, Japan.

Allen W. Glisson (S'71–M'78–SM'88–F'02) received the B.S., M.S., and Ph.D. degrees in electrical engineering from The University of Mississippi, University, in 1973, 1975, and 1978, respectively.

In 1978, he joined the faculty of The University of Mississippi, where he is currently a Professor and Chair of the Department of Electrical Engineering. His current research interests include the development and application of numerical techniques for treating electromagnetic radiation and scattering problems, and modeling of dielectric resonators and dielectric-resonator antennas. He is an Associate Editor for *Radio Science*, and Co-Editor-in-Chief of the *Applied Computational Electromagnetics Society Journal*.

Dr. Glisson is a member of Commission B of URSI and the Applied Computational Electromagnetics Society. Since 1984, he has served as the associate editor for book reviews and abstracts for the *IEEE Antennas and Propagation Society Magazine*. He recently served as the editor-in-chief of the IEEE TRANSACTIONS ON ANTENNAS AND PROPAGATION. He currently serves on the Board of Directors of the Applied Computational Electromagnetics Society and is a member of the IEEE Antennas and Propagation Society (IEEE AP-S) Press Liaison Committee. He previously served as a member of the IEEE AP-S Administrative Committee (AdCom) and as the secretary of Commission B of the U.S. National Committee of URSI. He was selected as the Outstanding Engineering Faculty Member in 1986, 1996, and 2004. He was the recipient of the 1989 Ralph R. Teetor Educational Award and 2002 Faculty Service Award of the School of Engineering. He was also the recipient of a Best Paper Award presented by the SUMMA Foundation. He twice received a citation for excellence in refereeing from the American Geophysical Union. He was a recipient of the 2004 Microwave Prize presented by the IEEE Microwave Theory and Techniques Society (IEEE MTT-S).